

# In Situ Kinetics Reveal the Influence of Solvents and Monomer Structure on the Anionic Ring-Opening Copolymerization of Epoxides

Philip Dreier, Rebecca Matthes, Ramona D. Barent, Sandra Schüttner, Axel H. E. Müller,\* and Holger Frey\*

Dedicated to Brigitte Voit on the occasion of her 60th birthday

**In-depth understanding of copolymerization kinetics and the resulting polymer microstructure is crucial for the design of materials with well-defined properties. Further, insights regarding the impact of solvents on copolymerization kinetics allows for precisely tuned materials. In this regard, in situ  $^1\text{H}$  NMR spectroscopy enables precise monitoring of the living anionic ring-opening copolymerization (AROP) of ethylene oxide (EO) with the glycidyl ethers allyl glycidyl ether (AGE) and ethoxy vinyl glycidyl ether (EVGE), respectively. Determination of reactivity ratios reveals slightly higher reactivity of both glycidyl ethers compared to EO, emphasizing a pronounced counterion chelation effect by glycidyl ethers in AROP. Implementation of density functional theory (DFT) calculations further illustrates the complexation capability of ether-containing side groups in glycidyl ethers, in analogy to crown ethers (“crown ether effect”). Investigation of the copolymerization in i) THF- $d_8$  and ii) DMSO- $d_6$  shows an increasing disparity of reactivity ratios for both glycidyl ethers compared to EO, clearly related to decreasing solvent polarity.**

## 1. Introduction


In depth kinetic studies of the statistical copolymerization of different monomers have received renewed interest in recent years, particularly for living polymerization techniques. In this case, reactivity ratios mirror the monomer gradients along the chain and thus “mapping” of the chain composition from initiator to

chain end is feasible. Besides controlled radical polymerization, living anionic polymerization (LAP) remains the most efficient method for the synthesis of well-defined copolymers with narrow molecular weight distributions and controlled monomer gradients. Detailed understanding of the compositional profile of the comonomers along the polymer chains is of key importance in gradient or tapered copolymers to adjust the thermal properties in bulk<sup>[1–6]</sup> and consequently to control the morphology<sup>[1,4,7]</sup> and properties of the resulting materials.

To date, common methods for the evaluation of reactivity ratios and the corresponding comonomer gradient in the copolymer chains formed have relied on the determination of the comonomer content at different stages of copolymerization. After termination at different stages of the reaction,<sup>[8,9]</sup> samples were analyzed by gas chromatography to determine residual monomer

content.<sup>[10]</sup> These monitoring techniques are time-consuming, often rather difficult to implement and may hold uncertainties due to missing reproducibility, since the data are obtained from different polymerization experiments. In comparison, triad analysis via  $^{13}\text{C}$  inverse gated (IG) spectroscopy<sup>[11,12]</sup> is a reliable method for the determination of the global microstructure, but a large variety of samples must be synthesized for correct assignment and evaluation of the corresponding triads. In addition, it is not possible to derive the gradient structure. More recently, in situ monitoring via near infrared (NIR) spectroscopy<sup>[7,13,14]</sup> was established as a feasible analytical tool to directly correlate the polymerization kinetics with the copolymer microstructure for carbanionic copolymerization. The in situ methods advantageously permit to follow the mean composition over the whole conversion range, that is, at all given chain positions, resulting in a full compositional profile of the copolymers.<sup>[7,15]</sup> For instance, the influence of temperature<sup>[7]</sup> and polar additives<sup>[13,14]</sup> on the compositional drift and steepness of the gradient in isoprene/styrene-based tapered block copolymers, synthesized via carbanionic copolymerization, was recently investigated in great detail via NIR spectroscopy.

P. Dreier, R. Matthes, R. D. Barent, S. Schüttner, A. H. E. Müller, H. Frey  
 Department of Chemistry  
 Johannes Gutenberg-University  
 Duesbergweg 10–14, D-55128 Mainz, Germany  
 E-mail: axel.mueller@uni-mainz.de; hfrey@uni-mainz.de

 The ORCID identification number(s) for the author(s) of this article can be found under <https://doi.org/10.1002/macp.202200209>

© 2022 The Authors. Macromolecular Chemistry and Physics published by Wiley-VCH GmbH. This is an open access article under the terms of the Creative Commons Attribution-NonCommercial-NoDerivs License, which permits use and distribution in any medium, provided the original work is properly cited, the use is non-commercial and no modifications or adaptations are made.

DOI: 10.1002/macp.202200209

The rather slow polymerization kinetics of the anionic ring-opening polymerization (AROP) in polar aprotic solvents facilitates NMR spectroscopic monitoring at room temperature. This has been exploited to follow the monomer consumption of epoxides<sup>[16–22,12,23]</sup> as well as activated aziridines<sup>[24–27]</sup> via in situ <sup>1</sup>H NMR spectroscopy. Depending on the comonomer employed, the copolymerization of EO with monosubstituted epoxides may result in rather different polymer microstructures. For instance, preferred addition of EO over alkylene oxides<sup>[19]</sup> and glycidyl amines<sup>[16]</sup> to the active chain end has been observed. In anionic copolymerization with EO, both propylene oxide ( $r_{EO} = 2.8$ ,  $r_{PO} = 0.25$ )<sup>[11]</sup> and butylene oxide ( $r_{EO} = 6.46$ ,  $r_{BO} = 0.148$ ) exhibit significantly lower reactivities compared to EO.<sup>[22]</sup> In contrast, the copolymerization of EO with various glycidyl ethers (GE) generally revealed an almost ideally random distribution of the comonomer units along the polyether backbone.<sup>[17,20,28,21]</sup> Considering the underlying reactivity ratios,  $r$ , and rate constants,  $k$  ( $r_{EO} = k_{EO,EO}/k_{EO,GE}$ ,  $r_{EO} = k_{GE,GE}/k_{GE,EO}$ ), this copolymerization behavior necessitates  $k_{EO,EO} = k_{GE,EO}$  as well as  $k_{GE,GE} = k_{EO,GE}$  and thus the product  $r_{EO} \cdot r_{GE}$  equals unity. Consequently, non-terminal models, for example, the Jaacks method<sup>[29]</sup> can be employed to investigate the underlying copolymerization kinetics in AROP.<sup>[28,23,17]</sup>

In addition to the chemical nature of the monomers, the polarity of the solvent and its potential interaction with the counterion affects the kinetics of AROP copolymerization. EO or substituted epoxides have been investigated with regard to polymerization kinetics in different aprotic polar solvents ranging from linear and cyclic ethers<sup>[30–33]</sup> to polar solvents like dimethyl sulfoxide (DMSO)<sup>[34–38]</sup> and hexamethylphosphoramide (HMPA).<sup>[36,39]</sup> Depending on the polarity of the solvents, ion pairs were observed as reactive species in ethers,<sup>[33,31]</sup> whereas free ions were found to be present in the case of the more polar DMSO<sup>[40]</sup> and HMPA.<sup>[39]</sup> Nevertheless, although the homopolymerization kinetics in these solvents is well understood, the influence of the solvent on the copolymerization kinetics of EO with monosubstituted epoxides remains largely unexplored.

In 2011, our group investigated the microstructure of copolymers consisting of ethoxy vinyl glycidyl ether (EVGE) and EO copolymerized with cesium alkoxides in THF via <sup>13</sup>C NMR triad analysis. The post-polymerization analysis revealed a random distribution of EVGE units along the polymer backbone while no specific reactivity ratios were calculated.<sup>[41]</sup> One year later, Lynd, Hawker and coworkers reported a novel initiator-based method for the calculation of the reactivity ratios based on post-polymerization <sup>1</sup>H NMR spectroscopy. Here, the AROP copolymerization of EO and monosubstituted epoxides, namely EVGE and allyl glycidyl ether (AGE), was investigated in THF with potassium alkoxides as active chain ends.<sup>[42]</sup>

To the best of our knowledge, merely the variation of the reactivity ratios in the presence of electron donors has been investigated in detail for the copolymerization of epoxides to date.<sup>[10]</sup> Further, online monitoring of the comonomer consumption during copolymerization of EO with EVGE/AGE has not been compared in-depth regarding the influence of substituents as well as solvent variation.

In the current work we utilize in situ <sup>1</sup>H NMR kinetics to evaluate and compare the reactivity ratios of the copolymerization of EO with EVGE and AGE, respectively, both in tetrahydrofuran-

$d_8$  (THF- $d_8$ ) and DMSO- $d_6$  as solvents (Scheme 1). DFT calculations were employed, leading to an in-depth understanding of the copolymerization kinetics.

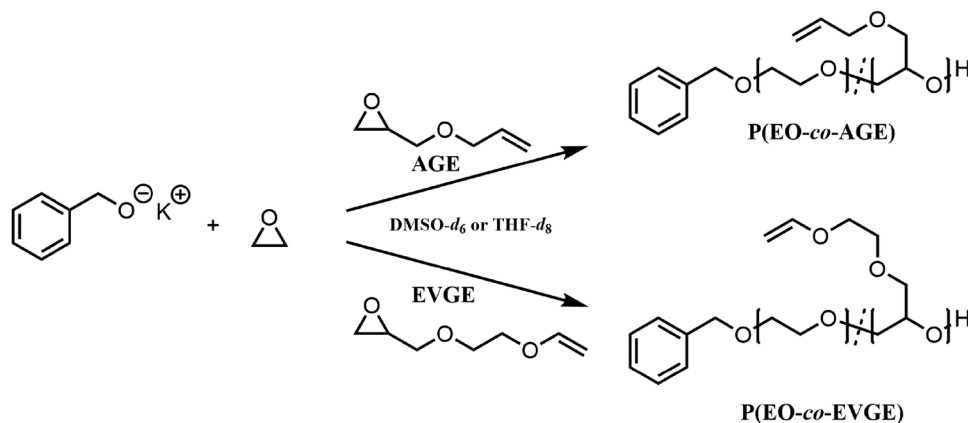
## 2. Results and Discussion

### 2.1. Impact of Solvents on Copolymerization Kinetics of EO and Glycidyl Ethers

The anionic ring-opening polymerization (AROP) of epoxides is often performed in polar solvents to achieve ion pair separation and consequently accelerate the polymerization. DMSO with a dipole moment of 3.96 D is the solvent with the highest polarity that can be utilized in AROP, besides the carcinogenic HMPA, which was not used in this study for safety reasons. Thus, DMSO can be considered as the ideal polar system with a high extent of ion dissociation and free ions as the active species.<sup>[40]</sup> On the contrary, THF exhibits a lower dipole moment of 1.63 D and accordingly is a less polar solvent implemented in AROP, permitting only partial dissociation of alkali metal alkoxides.<sup>[43]</sup> The reactive species of the alkoxide chain ends in THF can be characterized as ion pairs. These ion pairs are in equilibrium with unreactive aggregates,<sup>[31]</sup> and polymerization in THF most likely mimics the behavior in bulk polymerizations of epoxides. Therefore, DMSO and THF represent a strongly polar and a comparably nonpolar example to perform AROP of epoxides. Although several studies targeting the copolymerization of EO with various substituted epoxides have been conducted in either THF, DMSO, or mixtures of both, their influence on the copolymerization kinetics has not been compared in a detailed manner to date. Based on this lack of data, we elucidated the impact of solvent polarity on the incorporation of different epoxides in the polyether during the copolymerization of EO with monosubstituted epoxides via in situ <sup>1</sup>H NMR kinetics. To this end, model copolymerization reactions of EO with the two typical glycidyl ethers AGE and EVGE, respectively were performed, initiated by potassium benzyl alkoxide at 45°C in DMSO- $d_6$  and THF- $d_8$ , respectively. Potassium benzyl alkoxide was selected as initiator as a commonly employed example in AROP.<sup>[44,42]</sup> By recording one spectrum every 30 s, the monomer consumption was monitored over time (Figure 1, top),

As shown in Figure S1, Supporting Information, in DMSO, the copolymerization of EO with AGE and EVGE exhibits high propagation rates, with a half-life (50% conversion) of the respective glycidyl ether of 13 (AGE) and 20 min (EVGE), respectively. A plot of comonomer consumption versus total conversion, as shown in Figure 1 (bottom), shows that in both cases the glycidyl ether is incorporated slightly faster than EO.

Implementation of the Jaacks equation<sup>[29]</sup> enabled the calculation of reactivity ratios for both copolymerizations with a coefficient of determination ( $R^2$ ) of 0.9995 (AGE) and 0.998 (EVGE), respectively (Figure S2, Supporting Information). The Jaacks model is a non-terminal, integrated model for ideal copolymerizations that originates in the simplification  $r_1 = r_2^{-1}$  and relies on the linearization of the Meyer–Lowry equation. The latter is applicable, if the rate of monomer incorporation does not show a strong dependence on the identity of the terminal unit, but on the nature of the reacting monomers. Its strength lies in the reduction of potential errors caused by overfitting. The implementation of the non-terminal model is further justified by DFT cal-



**Scheme 1.** Copolymerization for P(EO-co-AGE) and P(EO-co-EVGE), initiated by potassium benzyl alkoxide in DMSO-*d*<sub>6</sub> and THF-*d*<sub>8</sub>.

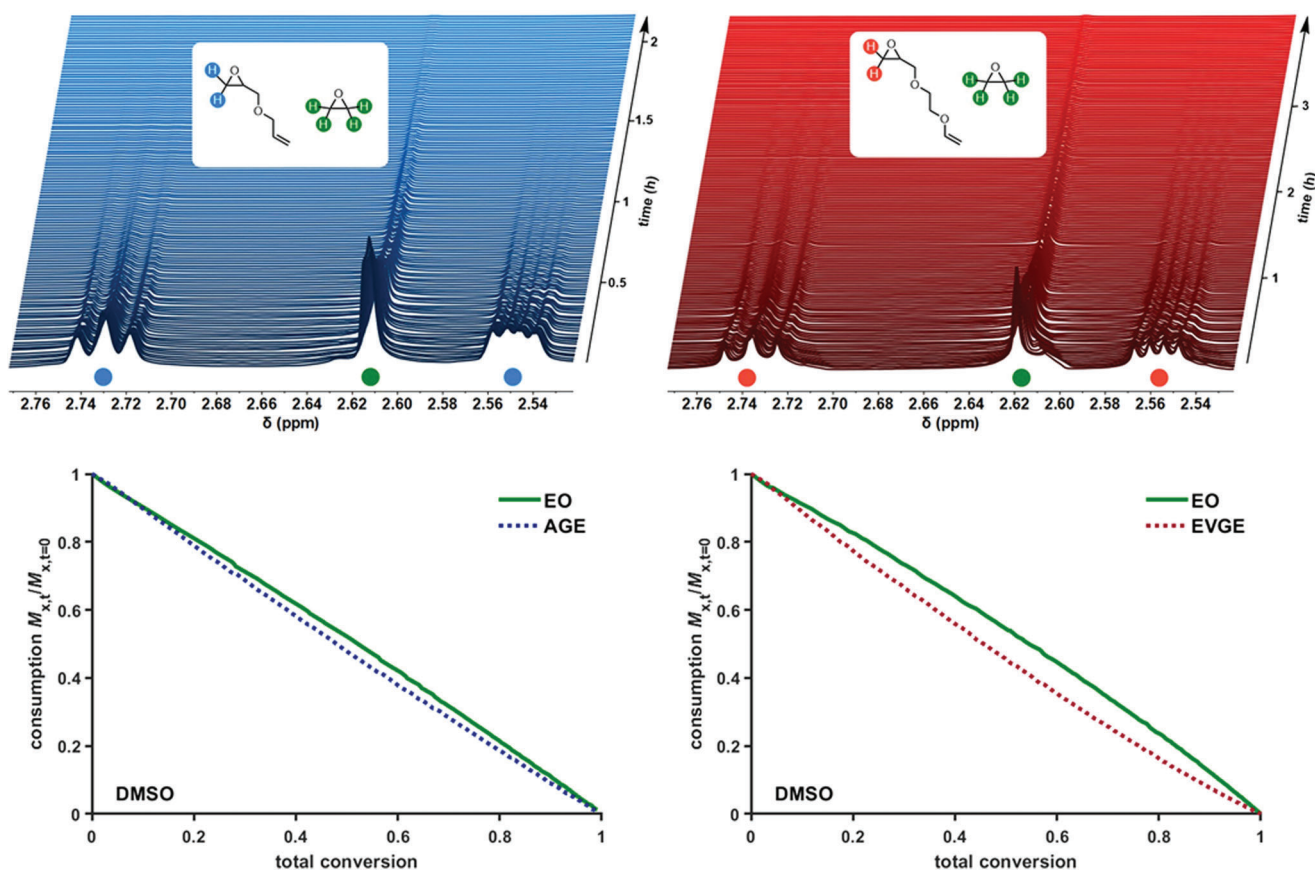


**Figure 1.** Top: in situ <sup>1</sup>H NMR kinetics of the anionic copolymerization of EO with AGE in DMSO-*d*<sub>6</sub> (left) and with EVGE (right), initiated by potassium benzyl alkoxide at 45 °C; bottom: conversion of both comonomers versus total conversion.

culations, as discussed in a later section. Note that reactivity ratios are defined as  $r_1 = k_{1,1}/k_{1,2}$  and  $r_2 = k_{2,2}/k_{2,1}$  with index 1 representing EO and 2 the respective glycidyl ether. Both glycidyl ethers demonstrate rate constants of  $k_{\text{AGE,AGE}} > k_{\text{AGE,EO}}$  and  $k_{\text{EVGE,EVGE}} > k_{\text{EVGE,EO}}$ , resulting in the preferential incorporation of AGE and EVGE in the early stages of the copolymerization. The herein performed in situ kinetic experiments in DMSO con-

sequently revealed reactivity ratios of  $r_{\text{EO}}^{\text{DMSO}} = 0.92 \pm 0.002$  and  $r_{\text{AGE}}^{\text{DMSO}} = 1.08 \pm 0.002$  as well as  $r_{\text{EO}}^{\text{DMSO}} = 0.81 \pm 0.001$  and  $r_{\text{EVGE}}^{\text{DMSO}} = 1.23 \pm 0.002$ . Collectively, the copolymerization of EO and AGE in DMSO shows nearly ideally random character, whereas the copolymerization with EVGE results in a very slight gradient microstructure. Based on the obtained reactivity ratios, the molar composition diagrams  $F_{\text{GE}}$  versus total conversion il-

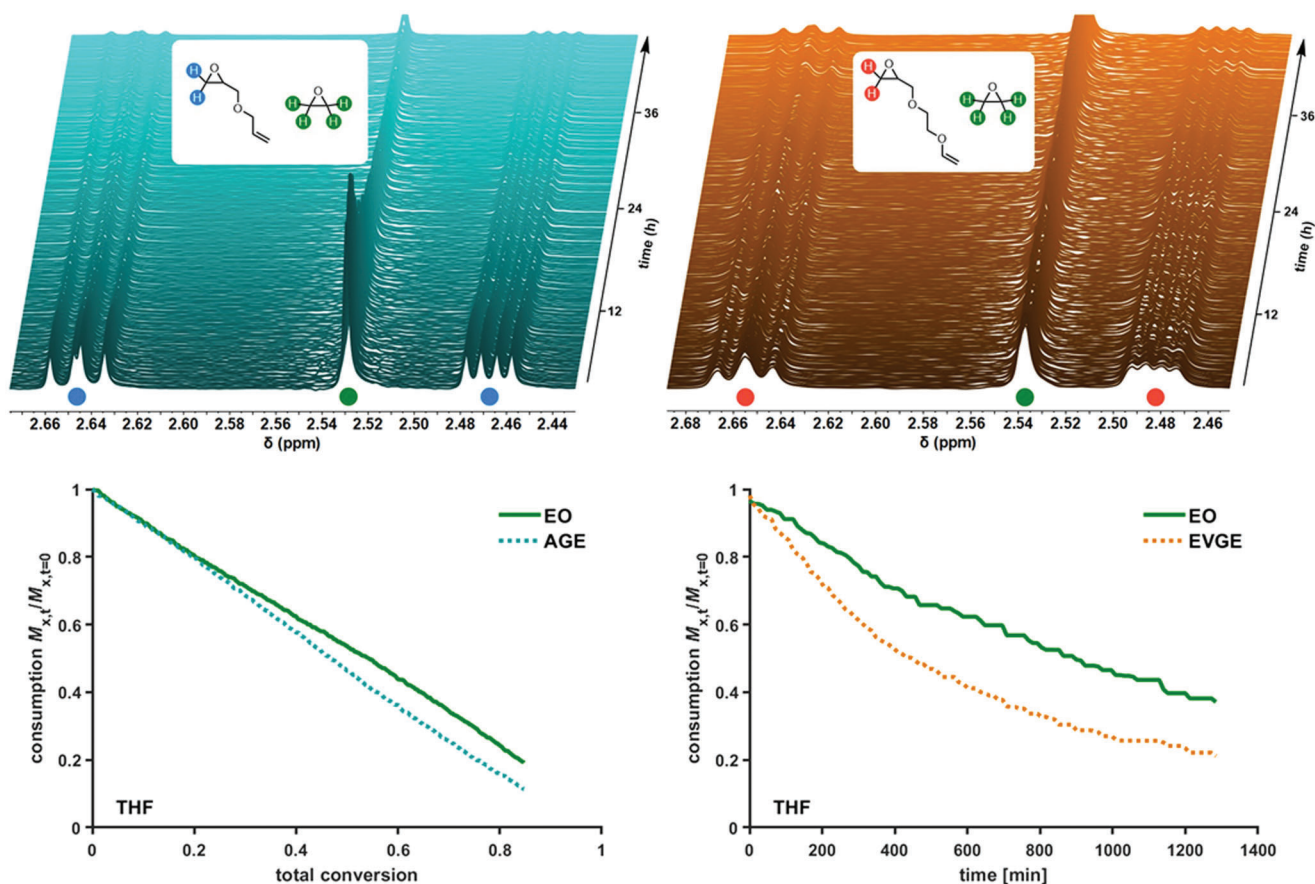


**Figure 2.** Top: in situ  $^1\text{H}$  NMR kinetics in THF- $d_8$  of the anionic copolymerization of EO/AGE (left) and EO/EVGE (right), initiated by potassium benzyl alkoxide at  $45^\circ\text{C}$ ; bottom: consumption  $M_{x,t}/M_{x,t=0}$  versus total conversion for P(EO-co-AGE) (left) and for P(EO-co-EVGE) (right).

illustrate the close to random (AGE) and slight gradient (EVGE) microstructure (Figure S3, Supporting Information).

Subsequently, analogous in situ  $^1\text{H}$  NMR kinetic experiments were performed in THF to determine the polymerization kinetics of ion pairs in equilibrium with unreactive aggregates. As expected, in THF both copolymerizations revealed significantly decreased propagation rates compared to DMSO, leading to half-lives of 17.3 h (AGE) and 7.6 h (EVGE), respectively (Figures 2 and Figure S4, Supporting Information). The experiment was not carried out to full conversion due to limited measurement time. Nevertheless, the amount of data points reaching  $>70\%$  conversion ensures a reliable evaluation of reactivity ratios by the Jacks equation ( $R^2$  of 0.997 (AGE) and 0.992 (EVGE)) (Figure S5, Supporting Information).

The differences in reactivity between EO and both glycidyl ethers are notably more pronounced in THF in comparison to the polar DMSO system, albeit without changing the overall trend. Accordingly, reactivity ratios were determined as  $r_{\text{EO}}^{\text{THF}} = 0.78 \pm 0.001$  and  $r_{\text{AGE}}^{\text{THF}} = 1.29 \pm 0.002$  as well as  $r_{\text{EO}}^{\text{THF}} = 0.48 \pm 0.004$  and  $r_{\text{EVGE}}^{\text{THF}} = 2.05 \pm 0.015$ . In THF, both copolymerizations exhibit soft gradient microstructures, illustrated in the molar composition diagrams (Figure S6, Supporting Information). In the case of P(EO-co-EVGE), the gradient determines the nature of the terminal units, consisting almost exclusively of EO repeating units, which can be important for further trans-

formation of the chain end. The investigated polymerizations in DMSO as well as THF resulted in polymers of low to moderate dispersities ( $\bar{D} < 1.19$ ) (see Figure S7, Supporting Information).

A summary of the evaluated reactivity ratios compared to the values reported by Lynd, Hawker and coworkers<sup>[42]</sup> based on a different method, that is, the end-group dyad (EGD) method as well as the current results of our group evaluated by  $^{13}\text{C}$  NMR triad analysis (for EVGE)<sup>[41]</sup> is given in Table 1. The reactivity ratios evaluated for the copolymerization of EO and AGE in THF are in good agreement for both methods (in situ and EGD), while the error is decreased for in situ kinetics due to the large amount of data points. However, the copolymerization of EO and EVGE shows a pronounced discrepancy when comparing the different methods. The EGD analysis yielded a more pronounced reactivity of EVGE compared to the established in situ method as well as the  $^{13}\text{C}$  NMR triad analysis. Analysis via EGD enables facile and quick first access to reactivity ratios subsequent to several polymerization experiments via  $^1\text{H}$  NMR spectroscopy, but it relies on the first monomer addition steps at the initiator. In contrast, in situ experiments reveal online results with a multitude of data points over minutes up to hours reaction time, however necessitating a demanding reaction set-up within the NMR spectrometer. Nevertheless, the calculated reactivity ratios are independent of the nature of the utilized initiator and enable precise results with low error values, notably up to full monomer conversion.

**Table 1.** Reactivity ratios evaluated by in situ  $^1\text{H}$  NMR experiments using the Jaacks method,<sup>[29]</sup> by EGD<sup>[42]</sup> and  $^{13}\text{C}$  triad analysis.<sup>[41]</sup>

Monomer	Method	Solvent	$r_{\text{EO}}$	$r_{\text{EO}}^{\text{err}}$	$r_{\text{GE}}$	$r_{\text{GE}}^{\text{err}}$	$r_{\text{EO}} \times r_{\text{GE}}$	$R^2$
AGE	Jaacks	DMSO	0.92	0.002	1.08	0.002	1.00	0.9995
	Jaacks	THF	0.78	0.001	1.29	0.002	1.00	0.997
	EGD	THF	0.54	0.03	1.31	0.26	0.71	-
EVGE	Jaacks	DMSO	0.81	0.001	1.23	0.002	1.00	0.998
	Jaacks	THF	0.48	0.004	2.05	0.015	1.00	0.992
	EGD	THF	0.32	0.10	3.50	0.90	1.12	-
	triad analysis	THF						$r_{\text{EO}} \approx r_{\text{GE}} \approx 1$

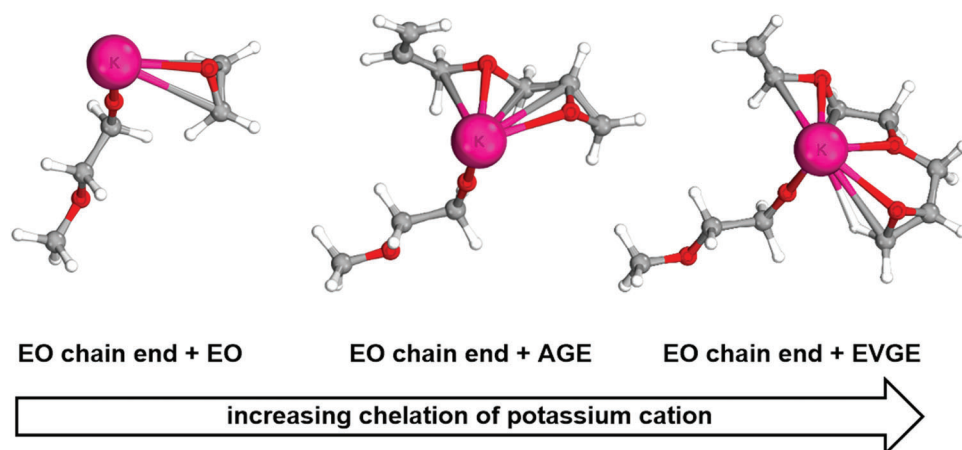


**Figure 3.** Complexation of potassium by EO chain end with EO, AGE, and EVGE calculated by DFT.

## 2.2. Impact of Transition State on Monomer Reactivity

The described results demonstrate that the influence of cation complexation on monomer reactivities during the polymerization is more pronounced in THF rather than DMSO. Following these findings, we postulate a transient “crown ether-effect” of the investigated glycidyl ethers, causing the enhanced reactivity of both glycidyl ethers compared to EO in THF, as also mentioned by Lynd, Hawker et al.<sup>[42]</sup> It is a known phenomenon that the addition of 18-crown-6, a cyclic oligo(ethylene glycol) consisting of six EO repeating units, strongly complexes potassium cations in THF.<sup>[45]</sup> The distance of two methylene units between the oxygens of 18-crown-6 is similarly found for the three oxygens in EVGE. Based on this rationale, a preferential combined complexation of the potassium cation with EVGE monomer and the alkoxide of the propagating chain via chelation can be hypothesized and investigated by quantum chemistry methods, namely density functional theory (DFT) (Figure 3, right). In contrast, EO exhibits only one coordination site per monomer and therefore a lower complex coordination constant with potassium cations. Consequently, this results in a higher probability to find EVGE rather than EO in the chain segments close to the initiator, explaining the preferential incorporation of EVGE ( $r_{\text{EVGE}} > r_{\text{EO}}$ ) during chain propagation. The chelation of potassium cations is less pronounced for AGE, as only two possible coordination sites are present in each AGE monomer (Figure 3, center). Therefore, the stability constant of AGE complexes is lower than that of EVGE,

but still somewhat higher than for EO, resulting in a merely slightly preferred addition of AGE to the chain end in THF ( $r_{\text{AGE}} > r_{\text{EO}}$ ).

The propagating chain ends of the three investigated monomers were simulated using DFT calculations. As visualized in Figure S8, Supporting Information, the presence of a glycidyl ether, namely AGE or EVGE, as an ultimate or penultimate repeating unit of the growing chain allows for a complexation by not merely the backbone oxygens of the former epoxide moiety, but also by the glycidyl ether’s side chain. In the case of AGE, the number of oxygens potentially coordinating to the potassium counterion equals the number of coordinating atoms when the backbone aligns with the counterion. On the contrary, with the two oxygen atoms of the side chain of EVGE, the propagation chain end with (pen)ultimate EVGE units further saturates the complexation sites of the potassium counter ion. As discussed, the coordination capability of the monomers to be added follows the trend  $\text{EO} < \text{AGE} < \text{EVGE}$  (Figure 3).

The enhanced coordination of the potassium counterion by the monomer going from EO and AGE to EVGE was observed as a local energy minimum. Hence, the inherent entropic benefit is a determining factor for the preferred chelation of the potassium cation. Furthermore, we compared the electron densities of the electrophilic methylene groups of the epoxides calculated by DFT, which are attacked by the alkoxide during polymerization. Since the bond angles of the different epoxides and hence the ring strain of the monomers are comparable, the electron density is

**Table 2.** Partial charges of the unsubstituted methylene carbon of the epoxide moiety of the monomers ethylene oxide (EO), allyl glycidyl ether (AGE), and ethoxy vinyl glycidyl ether (EVGE) calculated by DFT without taking solvation into account or rather in THF and DMSO using CPCM.

System	EO	AGE	EVGE
Vacuum	-0.285 e	-0.251 e	-0.251 e
THF	-0.275 e	-0.242 e	-0.249 e
DMSO	-0.273 e	-0.240 e	-0.243 e

the pivotal parameter for the monomer reactivity. In **Table 2**, the partial charges of the three monomers simulated in vacuum as well as in THF and DMSO are given, using the implicit solvation model CPCM.

Both investigated glycidyl ethers exhibit lower electron density at their electrophilic carbon relative to EO. The trend is further decreased for all epoxides with increasing dipole moment of the respective solvent. Consequently, the partial charges give a first indication for preferential incorporation of the glycidyl ethers at the chain end compared to EO. The observed trend in monomer reactivity is further verified by evaluating the electron densities of the electrophilic epoxide methylene groups once coordinated to the propagating chain end, (see Table S1, Supporting Information).

This is in accordance with the observed trend from the in situ  $^1\text{H}$  NMR kinetic experiments. Surprisingly, the unsubstituted methylene carbon of AGE exhibits a higher electrophilicity than the respective carbon of EVGE in all solvents. Considering the afore described reactivity ratios, the potassium complexation of glycidyl ethers appears to be the major contributing factor to the copolymerization kinetics in THF, rather than the electrophilicity itself. These findings suggest that the monomer, but not the respective chain, primarily affects the incorporation with its specific complexation behavior. This further supports the implementation of the non-terminal model for the determination of reactivity ratios by in situ  $^1\text{H}$  NMR measurements.

Additional considerations are required to understand the impact of solvent polarity on the differences of the reactivity ratios in THF and DMSO ( $r_{\text{GE}}^{\text{DMSO}}$  and  $r_{\text{GE}}^{\text{THF}}$ ). Compared to THF, DMSO is a solvent with a high dipole moment. The resulting high polarity of the solvent allows an excellent dissolution of ions. Therefore, free ions are the primary active species, which mainly contribute to propagation.<sup>[40]</sup> The strong solvation effect of DMSO has a documented impact on complexes, for example, it is known to decrease the stability constants of crown ether complexes.<sup>[46]</sup> This influence is clearly visible when comparing the reactivity ratios obtained via in situ  $^1\text{H}$  NMR measurements in the different solvents. In DMSO, only a slightly preferred incorporation of EVGE over EO is observed. Therefore, the previously proposed crown ether-effect of EVGE in THF (Figure 3) is less pronounced in the case of DMSO. This is additionally confirmed by the increasing  $r_{\text{EO}}$  values from THF (0.57) to DMSO (0.81) and the increasing similarity of  $r_{\text{EVGE}}^{\text{DMSO}}$  (1.23) and  $r_{\text{AGE}}^{\text{DMSO}}$  (1.08). The described influence of DMSO is equally observed in the copolymerization of EO with AGE, resulting in an almost ideally random copolymerization with  $r_{\text{EO}} \approx r_{\text{AGE}}$ . Similar values of the reactivity ratios were previously reported by our group for the

copolymerization of ethoxyethyl glycidyl ether (EEGE) with EO in DMSO under AROP conditions.<sup>[17]</sup>

In summary, variation of the chemical structure of a glycidyl ether, for example, the addition of an ethylene glycol spacer at the monomer side chain, has a distinct influence on the behavior of epoxide monomers in the copolymerization with EO and consequently the microstructure of the resulting copolymers. In this context, the choice of solvent thus has a pronounced effect on the copolymerization reaction kinetics.

Further, the choice of a non-polar solvent enables the synthesis of “EO-rich” terminal segments within the polymer microstructure. If post-modification of the  $\omega$ -terminus is desired, a decreased reactivity of EO in copolymerization leads to an increase of primary hydroxy functionalities in the resulting polyether. Consequently, the reactivity of the polyether copolymers for post-modification reactions is largely enhanced.

### 3. Conclusion

With this study we aim at a general understanding of the anionic ring-opening copolymerization kinetics of ethylene oxide (EO) with glycidyl ethers (GE), relying on online  $^1\text{H}$  NMR monitoring of the reaction. Allyl glycidyl ether (AGE) and ethoxy vinyl glycidyl ether (EVGE) were chosen as typical and synthetically valuable representatives of glycidyl ether monomers, and copolymerization was carried out either in THF or DMSO. Online  $^1\text{H}$  NMR kinetics enables in situ monitoring of monomer consumption, leading to precise and reliable determination of reactivity ratios by common non-terminal models. Both investigated glycidyl ethers exhibited slightly higher reactivity ratios than EO in DMSO as well as in THF. However, the reactivity difference increased with reduced solvent polarity. These results further emphasize the crown ether effect and the underlying multidentate cation complexation as the driving force for the enhanced reactivity of glycidyl ethers compared to EO in the anionic copolymerization. The impact of the crown ether-like complexation consequently increased with reduced cation dissociation in less polar media going from DMSO to THF. Supplementary calculations by density functional theory (DFT) support the presented crown ether-effect, showing the stronger complexation with increasing number of oxygen atoms comparing EO with ethylene glycol spacer containing GEs (EO < AGE < EVGE).

Overall, the results disclose the underlying effects of the slightly preferred glycidyl ether incorporation over EO. This is crucial for the design of glycidyl ether-based copolymers since the resulting microstructure is tunable to a certain extent by choice of solvent as well as the introduction of ethylene glycol spacers in the monomer structures. The monomer gradient governs the behavior of the resulting materials in bulk or solution. In summary, this study provides in-depth insights in epoxide reactivity with respect to the design of the respective monomers as well as its solvent dependence. The results emphasize the vast value of in situ experiments for the control of chemical properties via precise tuning of polymer microstructures.

### Supporting Information

Supporting Information is available from the Wiley Online Library or from the author.

## Acknowledgements

P.D. and R.M. contributed equally to this work. The manuscript was written through contributions of all authors. All authors have given approval to the final version of the manuscript.

Open access funding enabled and organized by Projekt DEAL.

## Conflict of Interest

The authors declare no conflict of interest.

## Data Availability Statement

The data that support the findings of this study are available from the corresponding author upon reasonable request.

## Keywords

anionic ring-opening polymerization, copolymerization, epoxide monomers, in situ kinetics, polyethers

Received: June 28, 2022

Revised: July 27, 2022

Published online: September 1, 2022

- [1] M. Steube, T. Johann, E. Galanos, M. Appold, C. Rüttiger, M. Mezger, M. Gallei, A. H. E. Müller, G. Floudas, H. Frey, *Macromolecules* **2018**, *51*, 10246.
- [2] E. Grune, T. Johann, M. Appold, C. Wahlen, J. Blankenburg, D. Leibig, A. H. E. Müller, M. Gallei, H. Frey, *Macromolecules* **2018**, *51*, 3527.
- [3] P. Hodrokoukes, G. Floudas, S. Pispas, N. Hadjichristidis, *Macromolecules* **2001**, *34*, 650.
- [4] R. Lach, R. Weidisch, K. Knoll, *J. Polym. Sci. B Polym. Phys.* **2005**, *43*, 429.
- [5] N. Singh, M. S. Tureau, T. H. Epps, III, *Soft Matter* **2009**, *5*, 4757.
- [6] M. Thunga, U. Staudinger, B. K. Satapathy, R. Weidisch, M. Abdel-Goad, A. Janke, K. Knoll, *J. Polym. Sci. B Polym. Phys.* **2006**, *44*, 2776.
- [7] M. Steube, T. Johann, M. Plank, S. Tjaberings, A. H. Gröschel, M. Gallei, H. Frey, A. H. E. Müller, *Macromolecules* **2019**, *52*, 9299.
- [8] A. A. Korotkov, G. V. Rakova, *Polym. Sci. U.S.S.R.* **1962**, *3*, 990.
- [9] C. C. Price, Y. Atarashi, R. Yamamoto, *J. Polym. Sci. A-1 Polym. Chem.* **1969**, *7*, 569.
- [10] A. Stolarzewicz, H. Becker, G. Wagner, *Acta Polym.* **1980**, *31*, 743.
- [11] F. Heatley, G.-a.-E. Yu, C. Booth, T. G. Blease, *Eur. Polym. J.* **1991**, *27*, 573.
- [12] V. S. Reuss, B. Obermeier, C. Dingels, H. Frey, *Macromolecules* **2012**, *45*, 4581.
- [13] M. Steube, T. Johann, H. Hübner, M. Koch, T. Dinh, M. Gallei, G. Floudas, H. Frey, A. H. E. Müller, *Macromolecules* **2020**, *53*, 5512.
- [14] J. M. Kim, S. B. Chakrapani, B. S. Beckingham, *Macromolecules* **2020**, *53*, 3814.
- [15] A. Natalello, M. Werre, A. Alkan, H. Frey, *Macromolecules* **2013**, *46*, 8467.
- [16] B. Obermeier, F. Wurm, H. Frey, *Macromolecules* **2010**, *43*, 2244.
- [17] J. Herzberger, D. Leibig, J. C. Liermann, H. Frey, *ACS Macro Lett.* **2016**, *5*, 1206.
- [18] J. Herzberger, D. Kurzbach, M. Werre, K. Fischer, D. Hinderberger, H. Frey, *Macromolecules* **2014**, *47*, 7679.
- [19] J. Blankenburg, E. Kersten, K. Maciol, M. Wagner, S. Zorbakhsh, H. Frey, *Polym. Chem.* **2019**, *10*, 2863.
- [20] J. Blankenburg, K. Maciol, C. Hahn, H. Frey, *Macromolecules* **2019**, *52*, 1785.
- [21] K. Niederer, C. Schüll, D. Leibig, T. Johann, H. Frey, *Macromolecules* **2016**, *49*, 1655.
- [22] W. Zhang, J. Allgaier, R. Zorn, S. Willbold, *Macromolecules* **2013**, *46*, 3931.
- [23] P. Verkoyen, P. Dreier, M. Bros, C. Hils, H. Schmalz, S. Seiffert, H. Frey, *Biomacromolecules* **2020**, *21*, 3152.
- [24] T. Homann-Müller, E. Rieger, A. Alkan, F. R. Wurm, *Polym. Chem.* **2016**, *7*, 5501.
- [25] E. Rieger, A. Alkan, A. Manhart, M. Wagner, F. R. Wurm, *Macromol. Rapid Commun.* **2016**, *37*, 833.
- [26] E. Rieger, J. Blankenburg, E. Grune, M. Wagner, K. Landfester, F. R. Wurm, *Angew. Chem.* **2018**, *57*, 2483.
- [27] T. Gleede, J. C. Markwart, N. Huber, E. Rieger, F. R. Wurm, *Macromolecules* **2019**, *52*, 9703.
- [28] J. Herzberger, K. Fischer, D. Leibig, M. Bros, R. Thiermann, H. Frey, *J. Am. Chem. Soc.* **2016**, *138*, 9212.
- [29] V. Jaacks, *Makromol. Chem.* **1972**, *161*, 161.
- [30] T. C. Majdanski, J. Vitz, A. Meier, M. Brunzel, S. Schubert, I. Nischang, U. S. Schubert, *Polymer* **2018**, *159*, 86.
- [31] K. S. Kazanskii, A. A. Solovyanov, S. G. Entelis, *Eur. Polym. J.* **1971**, *7*, 1421.
- [32] N. V. Ptitsyna, V. K. Kazakevich, K. S. Kazanskii, *Polym. Sci. U. S. S. R.* **1977**, *19*, 3218.
- [33] A. A. Solov'yanov, K. S. Kazanskii, *Polym. Sci. U. S. S. R.* **1972**, *14*, 1186.
- [34] C. E. H. Bawn, A. Ledwith, N. R. McFarlane, *Polymer* **1967**, *8*, 484.
- [35] C. Bawn, A. Ledwith, N. McFarlane, *Polymer* **1969**, *10*, 653.
- [36] C. C. Price, M. K. Akkapeddi, *J. Am. Chem. Soc.* **1972**, *94*, 3972.
- [37] C. C. Price, D. D. Carmelite, *J. Am. Chem. Soc.* **1966**, *88*, 4039.
- [38] A. A. Solov'yanov, K. S. Kazanskii, *Polym. Sci. U. S. S. R.* **1972**, *14*, 1196.
- [39] J. E. Figueruelo, D. J. Worsfold, *Eur. Polym. J.* **1968**, *4*, 439.
- [40] K. S. Kazanskii, A. A. Solovyanov, S. A. Dubrovsky, *Makromol. Chem.* **1978**, *179*, 969.
- [41] C. Mangold, C. Dingels, B. Obermeier, H. Frey, F. Wurm, *Macromolecules* **2011**, *44*, 6326.
- [42] B. F. Lee, M. Wolffs, K. T. Delaney, J. K. Sprafke, F. A. Leibfarth, C. J. Hawker, N. A. Lynd, *Macromolecules* **2012**, *45*, 3722.
- [43] S. Penczek, M. Cypryk, A. Duda, P. Kubisa, S. Slomkowski, *Prog. Polym. Sci.* **2007**, *32*, 247.
- [44] A. Lee, P. Lundberg, D. Klinger, B. F. Lee, C. J. Hawker, N. A. Lynd, *Polym. Chem.* **2013**, *4*, 5735.
- [45] J. Ding, F. Heatley, C. Price, C. Booth, *Eur. Polym. J.* **1991**, *27*, 895.
- [46] V. P. Solov'ev, N. N. Strakhova, O. A. Raevsky, V. Rüdiger, H.-J. Schneider, *J. Org. Chem.* **1996**, *61*, 5221.